Experimental and Theoretical Studies of the Reaction of Al Atoms with OCS and CS_2

Miriam R. Pérez, Yasuyuki Ishikawa, and Brad R. Weiner*

Department of Chemistry, University of Puerto Rico, P.O. Box 23346, University Station, Río Piedras, Puerto Rico 00931

Received: May 1, 1997; In Final Form: July 17, 1997[⊗]

The temperature (295−382 K) and pressure (5−50 Torr) dependences of the rate constants of the Al + OCS and Al + CS_2 reactions have been studied by using time-resolved laser-induced fluorescence spectroscopy. The temperature dependence of the Al + OCS reaction is characterized by the rate expression $k_{II}^{OCS} = (4.2 \pm 2.1) \times 10^{-11} \exp[5.3 \pm 1.4 \text{ kJ mol}^{-1}/RT]$ cm^3 molecule^{-1} s^{-1}. The rate expression for the former reaction was found to be independent of total pressure up to 50 Torr. The pressure dependent rate expression for the reaction of Al + CS_2 obeys $k_{III}^{CS2} = (1.2 \pm 0.3) \times 10^{-28}$ cm^6 molecule^{-2} s^{-1}. Ab initio correlated calculations have been performed to determine the relative stability of the Al−CS_2 and Al−OCS collision complexes as well as the relative energetics of reactants and products.

Introduction

Recent breakthroughs in interdisciplinary fields, such as materials science[1] and fuel technologies,[2] have demonstrated the need for a firm understanding of the chemistry of gas-phase metal species. In particular, the oxidation chemistry of open shell metals can provide much insight into a variety of surface effects, such as corrosion and catalysis.[3] The majority of the experimental studies done to date focus on the reaction kinetics or examine the spectroscopy of intermediate species trapped in a cold matrix.[4] While kinetic studies of open shell metal species have provided useful data, they do not necessarily reveal a complete mechanistic picture at the molecular level. Matrix-isolation experiments provide valuable structural information, but do not address many aspects of the reactivity under real world conditions. An all-encompassing approach, i.e. using multiple techniques, can give a deeper understanding of the reaction mechanism, but is not always possible at the experimental level. Another approach is to use experiment in conjunction with modern theoretical methods to yield complementary information and thus give a more comprehensive view of the reaction process. This is the strategy we have chosen here to gain a broader understanding of the mechanism of aluminum atom reactions with carbonyl sulfide and carbon disulfide. In addition, this interactive approach can provide a valuable confirmation of the two methods.

Group 13 metals have been increasingly used in the new semiconductor and superconductor technology, with aluminum having a key role in many of the latest devices. Many solid propellants and explosives contain aluminum,[2] and its prolific use as an additive in rocket fuel has deposited a trail of metal species, both ionic and neutral, in the atmosphere.[5] Recently, group 13 chemistry has become an active field of gas-phase research due to the feasibility of producing metal atoms by using laser ablation and/or laser photolysis of organometallic precursors. Most of the studies have been done on boron and aluminum atom reactions.[4] Kinetic studies of the gas-phase reactions of atomic boron with the oxidizers O_2, SO_2, CO_2, and N_2O have been reported by Sridharan et al.[6] Room-temperature rate constants were determined for the O_2 and SO_2 reactions to have a value of $(9 \pm 7) \times 10^{-12}$ and $(7 \pm 5) \times 10^{-12}$ in units of cm^3 molecule^{-1} s^{-1}. Upper limits for the rate constants at 298 K for the B + CO_2 and B + NO_2 reactions of 5×10^{-13} cm^3 molecule^{-1} s^{-1} were suggested. A subsequent study by DiGiuseppe et al.[7] measured rate constants of $(4.6 \pm 1.8) \times 10^{-11}$, $(1.1 \pm 0.4) \times 10^{-10}$, $(7.0 \pm 2.8) \times 10^{-14}$, and $(2.1 \pm 0.8) \times 10^{-14}$ cm^3 molecule^{-1} s^{-1} for the O_2, SO_2, CO_2, and N_2O reactions at 298 K, respectively. Rate constants for boron atom reactions with other small molecules, such as H_2O, H_2O_2, alcohols, ethers,[8] and halomethanes,[9] have also been measured. Boron reactions have also been studied in rare gas matrixes in order to trap transient species and characterize them by FTIR spectroscopy.[10] For the B + O_2 reaction, the principal products were B_2O_2 and B_2O_3.[11] Complexes of boron with carbon monoxide,[12] acetylene,[13] methane,[14] nitrogen,[15] carbon dioxide,[16] and hydrogen[17] have also been detected. Quantum chemical calculations have isolated metastable structures and vibrational frequencies for the majority of the reaction intermediates.[13,15,16] Binding energies have been also reported for some of the complexes. Similar studies have been performed on the other members of group 13: aluminum,[20] gallium,[21] indium,[22] and thallium.[23]

The majority of the above studies have focused on the oxidation of the metal and have been motivated primarily by the capacity of reduced group 13 compounds as potential lightweight fuels or fuel additives. One reaction that has received a lot of attention has been the oxidation of aluminum by carbon dioxide,

$$\text{Al} + \text{CO}_2 \rightarrow \text{Products} \qquad (1)$$

In 1977, Fontijn et al. used a high-temperature fast flow reactor (HTFFR) to obtain the rate constant of the above reaction.[24] They observed a pronounced curvature of the Arrhenius plot at high temperatures ($T > 750$ K) and proposed that this could be due to the opening of a second product channel at high temperatures. Gole and co-workers found evidence of an $AlCO_2$ association complex by studying the oxidation reactions of Al atoms entrained in Ar, CO, and CO_2.[25] Parnis et al. determined the rate constant of the reaction to be pressure dependent in the range (10−600) Torr and the LIF signal of the AlO product to vary inversely with total pressure.[26] A mechanism involving the formation of an energized complex that can decompose to products or be stabilized by collisions was proposed. The pressure and temperature dependence of the rate constant of reaction (1) was also measured by Garland

* To whom correspondence should be addressed.
[⊗] Abstract published in *Advance ACS Abstracts,* November 1, 1997.

S1089-5639(97)01485-0 CCC: $14.00

et al.[27] Their reported rate constant exhibited a strong pressure dependence up to 700 K, where it became pressure independent. They concluded that at ambient temperatures the reaction proceeds by formation of an energized complex, with a rate constant $k = (5.6 \pm 1.3) \times 10^{-12} \exp((2.00 \pm 0.67)\ \text{kJ mol}^{-1}/\text{RT})\ \text{cm}^3\ \text{molecule}^{-1}\ \text{s}^{-1}$, whereas at temperatures above 700 K, direct O atom abstraction to produce AlO + CO is the primary channel. Other studies, both experimental and theoretical,[28−30] performed on this reaction support the existence of a long-lived $AlCO_2$ collision complex at room temperature.

Despite the strong interest in the reaction of Al with CO_2, the chemistry of aluminum with the isovalent sulfur-containing species, e.g. OCS and CS_2, has received little attention. EPR spectroscopic measurements of the aluminum and gallium atom reactions with CS_2, performed in a rotating cryostat at 77 K, are the only mechanistic studies reported.[31] In those studies, Howard et al. found evidence for the formation of both Al and Ga atom complexes with CS_2 and proposed structures for them. These workers found a surprising dissimilarity between the reactivities of CO_2 and CS_2 toward Al atoms and suggested further studies to understand these differences.

We describe here the pressure and temperature dependences of the kinetics of the following reactions:

$$Al(^2P^o_{1/2}) + CS_2(X\ ^1\Sigma_g) \rightarrow \text{Products} \quad (2)$$

$$Al(^2P^o_{1/2}) + OCS(X\ ^1\Sigma_g) \rightarrow \text{Products} \quad (3)$$

Al atoms are produced by the 248 nm multiphoton dissociation of trimethylaluminum (TMA) and monitored by time-resolved laser-induced fluorescence (LIF) spectroscopy. The rates of the reactions are measured by monitoring the disappearance of the Al atoms as a function of OCS and CS_2 concentrations. The production of AlS and the absence of AlO as a product in these reactions have been spectroscopically confirmed. Ab initio correlated calculations have been performed in order to determine the structures and relative stabilities of the Al−CS_2 and Al−OCS collision complexes as well as the relative energetics of the reactants and products.

Experimental Section

Experimental Apparatus. The experimental arrangement used for these studies has been described in general terms, previously.[32] The photolysis (pump) and probe laser beams are collinearly directed into a reaction chamber that consists of a six-way stainless steel cross with extension arms along the laser propagation axis. The extension arms contain conical baffles to reduce scattered laser light and have UV−Suprasil windows to transmit the pump and probe beams. Buffer gas (Ar) flow is directed through the ports near the windows to prevent deposition of photolysis products. The Al atom precursor and the OCS or CS_2 gas mixtures are flowed through concentric stainless steel tubes, which enter on one side of the stainless steel cross. Flow rates of each gas are measured using a calibrated flow meter prior to entering the cell. Total pressure is measured with a capacitance manometer. Partial pressures of the reactants are calculated from the measured flow rates and the total pressure. Temperature dependent studies (295−385 K) are achieved by wrapping the entire reaction cell with heating tape and monitoring the temperature with a K-type thermocouple located inside the cell. Temperatures are stable to ±2 K. The unfocused laser-induced fluorescence is viewed by a high-gain photomultiplier tube that is situated at 90° relative to both lasers. The output of the photomultiplier tube is processed and averaged by a gated integrator and then digitized and sent to a computer for display, storage, and analysis.

Production and Monitoring of Al Atoms. TMA is photolyzed with the focused output of an excimer laser (Lambda Physik LPX205i) using the KrF transition (248 nm). Typical photolysis laser fluences are 0.15−0.30 J/cm^2. The Al atoms are monitored by laser-induced fluorescence by exciting the $4\ ^2S_{1/2} \leftarrow 3\ ^2P^o_{1/2}$ transition centered near 394.4 nm using the output of a Lambda Physik 3002 tunable dye (QUI) laser pumped by a Lambda Physik LPX205i excimer laser, and detected by the $4\ ^2S_{1/2} \rightarrow 3\ ^2P^o_{3/2}$ transition through a narrow band-pass filter (fwhm = 1 nm; centered at 396.2 nm; Andover Corp.) at 396.2 nm.

Reactants. Trimethylaluminum (97%; Aldrich Chemical Co.) is submitted to a minimum of three freeze−pump−thaw cycles prior to gas mixture preparation. Carbon disulfide (Allied Chemicals) is distilled and also subjected to freeze−pump−thaw cycles. OCS (97.5%; Matheson Gas Products) is used as received. Ar (Spectra Gases, UHP grade) is used as a buffer gas to prepare all the gas mixtures. Gas mixture concentrations are 0.1% for TMA and 2.0% for both CS_2 and OCS. Typical flow rates are 8.2 slpm of TMA/Ar, (10−70) sccm of CS_2/Ar or OCS/Ar, and (1−170) sccm of Ar flowed over the windows. It is necessary to passivate the reaction chamber every day, by adding and retaining about 5 Torr of pure TMA into the cell for about 20 min. Following this procedure, the Al atom LIF signal did not fluctuate more than 20% during the course of a day's experiments.

Theoretical Calculations. The Gaussian 94 suite of computer programs[33] is used to calculate an equilibrium geometry and a set of harmonic frequencies for each structure associated with a minimum on the ground doublet-state potential energy surface. Accurate total energies for reactants, for products, and for the calculated intermediate structures are also determined by employing the G-2 method.[34] Minimum energy structures and harmonic frequencies are determined by the unrestricted Hartree−Fock (UHF) and the second-order Møller−Plesset (MP2) electron correlation method based on the UHF reference state: A "frozen core" has been used to exclude the inner shell from the correlated MP2 calculations. 6-311+G* basis sets were used. The ab initio energies for reactants, products, and the calculated intermediate structures were determined at the complete fourth-order Møller−Plesset theory (MP4 SDTQ/6-311+G*) and modified by a number of corrections to take into account further G-2 theoretical refinements.[34] The modifications include a correction for higher polarization on non-hydrogen atoms [ΔE(2df)]; a correction for correlation effects beyond fourth-order perturbation theory [ΔE(QCI)]; a higher level correction [ΔE(HLC)] calculated from the best fit to the experimental atomization energies of 55 molecules for which the experimental values are well-determined; and a correction for the addition of a third d function to the nonhydrogen atoms [Δ]. The total electronic energy (E_e) is obtained by adding all the corrections to the MP4 SDTQ/6-311+G* energy calculated previously. To calculate the energy of the molecule at zero temperature (E_0), a zero-point correction [ΔE(ZPE)] is evaluated from the harmonic frequencies and added to E_e.

Results

Experimental Results. Prior to beginning the kinetics experiments, we verify the production of Al atoms following 248 nm multiphoton dissociation of TMA by recording an LIF excitation spectrum near 394 nm. The details of this multiphoton dissociation have been studied and are described elsewhere.[35] We observe a single line at 394.4 nm, which corresponds to the $4\ ^2S_{1/2} \leftarrow 3^2P^o_{1/2}$ transition of Al.[36]

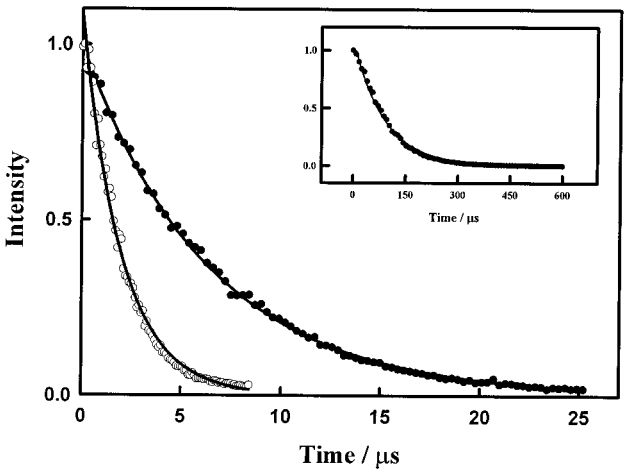

Figure 1. Typical transient profiles showing the decay of the Al LIF signal as a function of increasing delay time between the photolysis and probe laser pulses at two different total pressures for the following Al + CS_2 reaction conditions: (●) TMA = 5.7 mTorr, Ar = 10.7 Torr, CS_2 = 39.0 mTorr, total pressure = 10.73 Torr, τ = 6.2 μs; (○) TMA = 13.9 mTorr, Ar = 35.5 Torr, CS_2 = 85.5 mTorr, total pressure = 35.66 Torr, τ = 1.8 μs. The solid curve represents the best fit to a simple exponential decay rate. The inset illustrates the decay of the Al LIF signal in the absence of oxidant, where TMA = 5.2 mTorr and Ar = 10.8 Torr; τ = 82 μs.

Kinetic decay profiles of the Al atoms in the absence of any reactants are recorded at different total pressures and temperatures. Under these conditions, the single-exponential decay of the Al LIF signal (see Figure 1) is due to diffusion out of the probe laser beam and to reaction with TMA and/or photoproducts, yielding a nonreactive rate constant (k_b). The signal was not observed to grow in at short times, as has been reported in some previous studies.[27] The transients are obtained by monitoring the Al LIF signal at increasing probe laser delay times relative to the pump laser, which is controlled by a digital delay pulse generator. Nonreactive rate constants are obtained from the slope of a linear least-squares fit to the natural logarithm of each decay. Pseudo-first-order rate constants (k_I) are measured in a similar way after addition of a reactant (CS_2 or OCS). It is necessary to maintain k_b to be approximately an order of magnitude smaller than k_I, the pseudo-first-order rate constant, so that it is negligible in our analysis. To do so, the TMA pressure is minimized and the pressure of the reactant is increased until $k_b \ll k_I$. Pressure dependent studies are done by adding Ar to the desired level. Figure 1 shows typical kinetic decay profiles of the Al atom LIF signal in the presence of CS_2 at two different total pressures. Both of the temporal profiles can be fit adequately by a single-exponential decay.

To obtain second-order rate constants, k_{II}^{OCS} and k_{II}^{CS2} for reactions 2 and 3, the pseudo-first-order rate constants are plotted as a function of reactant partial pressure (Figure 2). The slope of the linear fit to this plot yields k_{II}. Following this procedure, the bimolecular rate constant for the Al + CO_2 reaction at 298 K and 10 Torr total pressure was measured and a value of (0.46 ± 0.04) × 10^{-12} cm^3 $molecule^{-1}$ s^{-1} was obtained, in excellent agreement with previous studies done on this reaction.[27] We have measured the total pressure and temperature dependences of the bimolecular rate constants for reactions 2 and 3, and the results are summarized in Tables 1 and 2.

The Arrhenius equation, often written as $k_{II} = Ae^{-E_a/RT}$, where A is the preexponential frequency factor and E_a is the activation energy, can be used to obtain mechanistic information about the reactions. Figure 3 shows a plot of k_{II} vs $1/T$ for the Al + OCS reaction. The points are fit by a least-squares method, and the slope of the line reveals a negative temperature

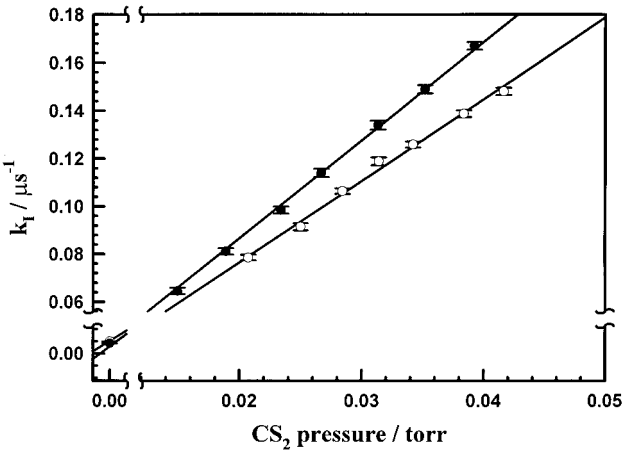

Figure 2. Plot of the variation in the pseudo-first-order rate constant as a function of CS_2 pressure at two different total pressures: (○) Total pressure is 15 Torr; (●) total pressure is 20 Torr. Temperature = 295 K. The lines are linear least-squares fits to the data points. Error bars are 2σ.

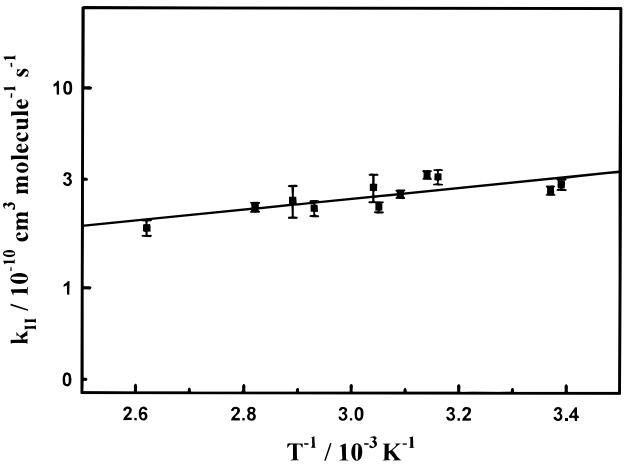

Figure 3. Arrhenius plot for the Al + OCS reaction. Temperature ranges from 295 to 382 K, and the total pressure is 10 Torr. The line is a linear least-squares fit to the data. Error bars are 2σ.

dependence. The reaction can be characterized by the following Arrhenius expression: $k_{II}^{OCS} = (4.2 \pm 2.1) \times 10^{-11} \exp[5.3 \pm 1.4 \text{ kJ mol}^{-1}/RT]$ cm^3 $molecule^{-1}$ s^{-1}. A temperature dependence was measured for the Al + CS_2 reaction at 10 Torr total pressure. As in the OCS case, a slightly negative temperature dependence was observed, but no Arrhenius expression is reported since the reaction is found to be pressure dependent (vide infra).

Pressure (Ar) dependence studies show that the bimolecular rate constant for reaction 2 increases monotonically over the range 5−45 Torr (Figure 4). The third-order rate constant, using argon as the buffer gas, is $k_{III} = (1.2 \pm 0.3) \times 10^{-28}$ cm^6 $molecule^{-2}$ s^{-1}. Similar experiments for the Al + OCS reaction reveal k_{II}^{OCS} to be pressure independent within experimental error over the range 5−50 Torr. The intercepts for k_I vs reactant pressure are found to decrease monotonically as a function of increasing pressure and even become slightly negative for higher total pressures, beginning at 20 Torr.

Theoretical Results. The starting point in our computational work to arrive at a metastable intermediate (in the case of both Al + OCS and Al + CS_2) was the structures that resemble the minimum energy $AlCO_2$ complexes calculated by Sakai.[29] For both reactions, we find minimum energy structures that correspond to Al−OCS and Al−SCS complexes in the potential energy surfaces. Figure 5a,b shows the optimized geometries

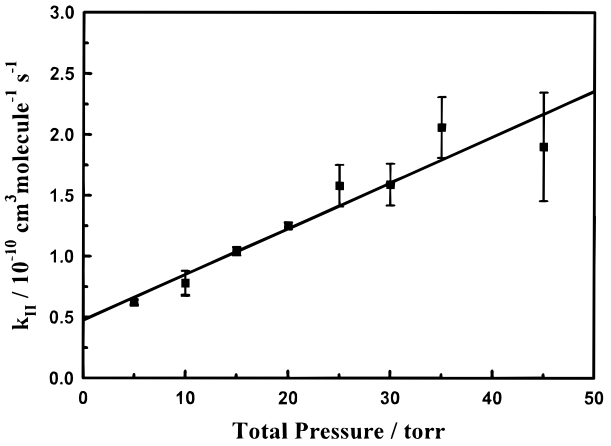

Figure 4. Plot of the bimolecular rate constant as a function of total pressure for the Al + CS_2 reaction. The line represents a linear least-squares fit to the data. Error bars are 2σ.

TABLE 1: Temperature and Pressure Dependence of the Bimolecular Rate Constant for the Al + CS_2 Reaction

T (K)	pressure (Torr)	$k_{II}^{CS2} \pm 2\sigma$ ($\times 10^{-11}$ cm^3 molecule^{-1} s^{-1})
295	5	6.2 ± 0.2
295	10	7.8 ± 1.0
295	10	7.8 ± 1.0
295	15	10.4 ± 0.4
295	20	12.5 ± 0.3
295	25	15.8 ± 1.7
295	30	15.9 ± 1.7
295	35	20.6 ± 2.5
295	45	19.0 ± 4.5
308	10	5.5 ± 0.5
319	10	4.6 ± 0.5
328	10	5.9 ± 0.8
334	10	5.2 ± 0.6
344	10	4.9 ± 0.6
359	10	4.7 ± 0.6
376	10	3.9 ± 0.4
377	10	3.5 ± 0.4

TABLE 2: Temperature and Pressure Dependence of the Bimolecular Rate Constant for the Al + OCS Reaction

T (K)	pressure (Torr)	$k_{II}^{OCS} \pm 2\sigma$ ($\times 10^{-10}$ cm^3 molecule^{-1} s^{-1})
295	5	3.6 ± 0.2
295	10	3.3 ± 0.2
295	20	3.2 ± 0.3
295	30	3.1 ± 0.3
295	45	3.4 ± 0.3
295	50	2.9 ± 0.4
297	10	3.1 ± 0.2
316	10	3.6 ± 0.3
318	10	3.7 ± 0.2
324	10	3.0 ± 0.1
328	10	2.6 ± 0.2
329	10	3.2 ± 0.5
341	10	2.5 ± 0.2
346	10	2.8 ± 0.5
355	10	2.5 ± 0.1
382	10	2.0 ± 0.2

for the AlSCO and AlSCS complexes. Table 3 and Figure 6 show the ab initio energies and G-2 theoretical energy corrections of the species involved in reactions 2 and 3. Table 4 shows the calculated harmonic frequencies for each complex.

Discussion

Al + OCS. Aluminum atoms can react by an abstraction reaction with OCS to produce either AlS + CO or AlO + CS. The latter reaction is endothermic and therefore thermodynamically less favored than the exothermic pathway that leads to AlS + CO (see Figure 6). The near gas kinetic rate obtained here for the disappearance of Al atoms in the presence of OCS suggests an exothermic pathway with a negligible activation barrier. The production of AlS was verified by exciting its A $^2\Sigma^+ - $X $^2\Sigma^+$ transition and recording the LIF spectrum in the 427.5−429.5 nm region. The obtained spectrum agrees with the previously reported AlS spectrum[37] and corroborates that the exothermic channel is operative. Previous experiments in our laboratory have monitored AlO laser-induced fluorescence.[38] In the experiment reported here, we have looked for the LIF spectrum of AlO (A $^2\Sigma^+ - $X $^2\Sigma^+$ transition) near 465 nm, but did not observe any signal, indicating that the endothermic channel is not occurring to any significant extent.

The enthalpy values for the reactions described above are taken from known experimental literature values[39] and agree well with those calculated here by the G-2 method. The G-2 method has been shown to be accurate for enthalpy values to within 12 kJ/mol for a large number of chemical compounds.[34] The slightly negative temperature dependence (see Figure 3) of this reaction is indicative of a negligible activation barrier. This effect can be understood if the reaction proceeds through a bound complex or adduct, which is separated from the final products by a small potential barrier.[40] Adducts are typically vibrationally excited species that are able to survive for at least several vibrations and can be collisionally stabilized. If no stabilization occurs, the adduct dissociates back into reactants or proceeds on to products. These two alternatives can be tested experimentally by recording the effect of total pressure on the rate of the reaction.

Studies measuring the bimolecular rate constant for this reaction as a function of total pressure show k_{II} to be pressure independent over the range measured (5−50 Torr). This suggests that the reaction is not proceeding through a collision complex. However, our calculations reveal a minimum in the potential energy surface corresponding to an AlSCO complex (see Figure 5b). One plausible explanation for this discrepancy would be that the potential well is shallow; that is, the barrier between complex and products is small. The extrapolated zero-pressure rate constant for Al + OCS is $(3.5 \pm 0.1) \times 10^{-10}$ cm^3 molecule^{-1} s^{-1}.

At the photolysis fluences used in this study, production of atoms by either single or multiphoton dissociation of OCS is a possibility. For this reason, we need to consider the possibility that the rate constant observed for the disappearance of Al atoms is due to reaction with S atoms instead of OCS. The observed room-temperature bimolecular rate constant is on the order of 3×10^{-10} cm^{3}molecule^{-1} s^{-1}, which is essentially gas kinetic. If the observed reaction rate were due to an S atom reacting with the Al instead of OCS, then approximately all of the carbonyl sulfide molecules would have to be dissociating. For the single-photon photodissociation of OCS (σ_{248} = ca. 10^{-20} cm^2/molecule[41]) at 248 nm, even at the high fluences used in this experiment, we do not expect more than 5% dissociation of the triatomic species. Assuming even 10% dissociation, we would obtain a rate constant for the Al + S → AlS reaction to be an order of magnitude higher than gas kinetic and therefore rule out this possibility. For the multiphoton dissociation scenario, we cannot accurately calculate the percent dissociation of the OCS species, but we expect it to be lower than the single-photon photodissociation.

Theoretical calculations show the energy on going from the complex to the products to be −12.1 kJ/mol. A binding energy of 81.9 kJ/mol for the AlSCO complex was calculated.

TABLE 3: Complete Fourth-order Møller−Plesset Energies (MP4 SDTQ/6-311+G*) and G-2 Theoretical Energy Corrections for the Species Involved in Reactions 2 and 3 (in au)

	MP4/6-311+G*	ΔE(2df)	ΔE(QCI)	ΔE(HLC)	ΔE(ZPE)	Δ_2	1.14 npair	$E_0(G_2)$
Al	−241.915 556	−0.007 856	-1.886×10^{-3}	-6.33×10^{-3}	0	-4.470×10^{-4}	1.14×10^{-3}	−241.930 935
CS_2	−833.384 265	−0.115 143	7.685×10^{-3}	-49.12×10^{-3}	6.132×10^{-3}	-8.139×10^{-3}	9.12×10^{-3}	−833.533 730
$AlCS_2$	−1075.333 533	−0.128 022	4.340×10^{-4}	-55.45×10^{-3}	7.548×10^{-3}	-7.952×10^{-3}	10.26×10^{-3}	−1075.506 715
AlS	−639.651 7497	−0.061 389	-2.918×10^{-3}	-24.75×10^{-3}	1.604×10^{-3}	-3.196×10^{-3}	4.56×10^{-3}	−639.737 839
CS	−435.626 794	−0.060 525	3.692×10^{-3}	-30.70×10^{-3}	3.014×10^{-3}	-4.962×10^{-3}	5.70×10^{-3}	−435.710 575
OCS	−510.808 608	−0.108 029	8.808×10^{-3}	-49.12×10^{-3}	7.967×10^{-3}	-9.022×10^{-3}	9.12×10^{-3}	−510.948 884
AlOCS	−752.747 645	−0.120 357	1.978×10^{-3}	-55.45×10^{-3}	8.930×10^{-3}	-8.725×10^{-3}	10.26×10^{-3}	−752.911 009
CO	−113.102 205	−0.053 545	4.800×10^{-3}	-30.70×10^{-3}	4.839×10^{-3}	-6.687×10^{-3}	5.70×10^{-3}	−113.177 798

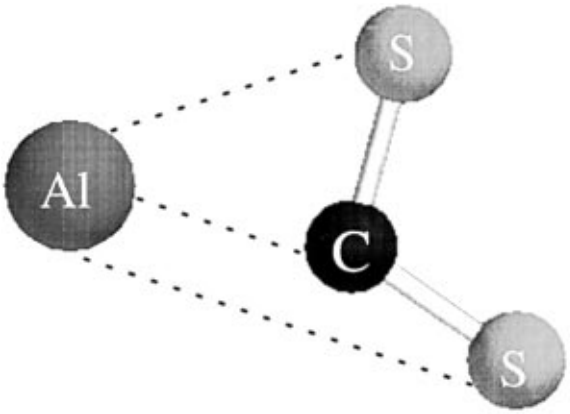

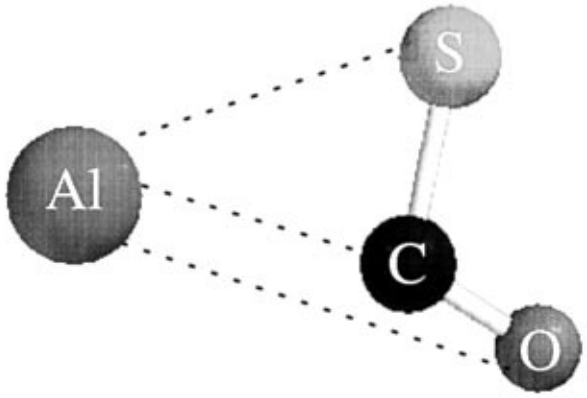

Figure 5. Optimized minimum energy geometries for (a) the AlSCS collision complex ($r_{AlS1} = 3.50$ Å, $r_{AlS2} = 2.40$ Å, $r_{AlC} = 2.19$ Å, $r_{CS1} = 1.59$ Å, $r_{CS2} = 1.67$ Å, $\angle S_1CS_2 = 148°$, $\angle AlCS_2 = 76°$) and (b) the AlSCO collision complex ($r_{AlS} = 2.38$ Å, $r_{AlO} = 3.25$ Å, $r_{AlC} = 2.19$ Å, $r_{CS} = 1.71$ Å, $r_{CO} = 1.19$ Å, $\angle SCO = 140.6°$, $\angle AlSC = 62°$).

Harmonic frequencies for the Al−OCS complex have been calculated at the MP2 level of theory and are shown in Table 4. Approximate descriptions of the normal-mode frequencies have been determined on the basis of comparison with similar systems.[29] When the results of the Al−OCS complex are compared with known values for free OCS, a general trend is observed where the harmonic frequencies are reduced, consistent with less electron density along the bond axis of carbonyl sulfide.

Mitchell et al. reported a procedure to obtain useful mechanistic information from a reaction with an observed negative temperature dependence, which in turn can be compared with

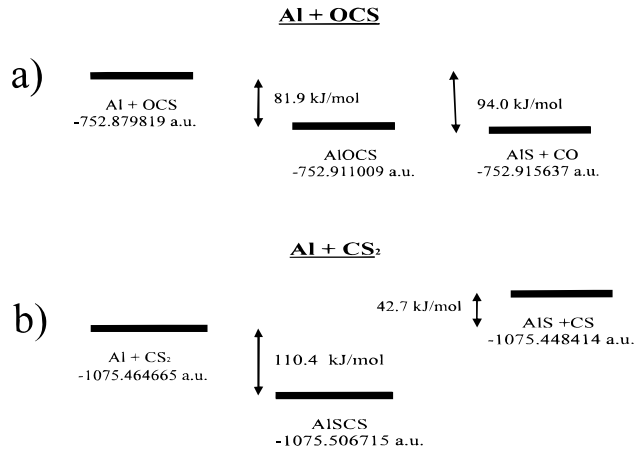

Figure 6. Relative electronic energies of the reactants, products, and collision complexes for (a) Al +OCS and (b) Al + CS_2.

our calculated values.[42] In their method, a lower limit to the binding energy associated with an intermediate complex can be estimated from the experimental rate constant and an assumed association rate constant. The results of their model using our experimental rate constants and an association rate constant of 10^{-9} cm^3s^{-1} give a lower limit to the binding energy of 10.6 kJ/mol for the Al−OCS complex. This value is significantly different from our calculated value of 81.9 kJ/mol. To the degree that this model is applicable, such a discrepancy could arise from a large barrier between the intermediate complex and the products, but this is inconsistent with our observed lack of pressure dependence for the reaction. Previous comparisons of calculated binding energies with experimental estimates have also shown significant discrepancies.[29]

As was mentioned in the Results section (see above), we observe a decrease in the *y*-intercept of the k_I vs reactant pressure plots (see Figure 2) as a function of increasing total pressure. At total pressures greater than 20 Torr, the intercepts are found to be negative. Obviously, this has no physical meaning and may arise from forcing a line through a second-order function. The second-order function stems from the fact that the rate expression for the Al + OCS reaction may be third order instead of second order, with carbonyl sulfide acting as both reactant and buffer. Once again, this apparent discrepancy can be understood in terms of a shallow potential well. This could result in a slight pressure dependence, which we were not able to detect in our rate constant measurements. We have not attempted to fit our data by higher order functions, because the correlation coefficients for the linear fits were high, i.e. $r^2 > 0.99$ in most cases. Experiments are currently underway at higher sensitivities to be able to measure these rate constants at lower reactant pressures and with more efficient colliders as buffers.

Al + CS_2. The thermodynamics of the reaction of $Al(^2P^o_{1/2})$ + $CS_2(X\ ^1\Sigma^+)$ to produce $AlS(X\ ^2\Sigma^+)$ + $CS(X\ ^1\Sigma^+)$ warrants some discussion (see Figure 6). If we use the heat of formation values for the reactants and products from the JANAF tables,

TABLE 4: Harmonic Frequencies for the AlSCS and AlSCO Complexes Determined at the MP2 Level of Theory (in cm^{-1})

mode	Al−CS_2 frequency	approximate[a] description	Al−OCS frequency	approximate[a] description
ω_1	159.6		210.7	
ω_2	295.8	S−Al−C bending	312.2	S−Al−C bending
ω_3	323.7	out of plane S−C−S bending	347.1	out of plane O−C−S bending
ω_4	440.2	in plane S−C−S bending	501.1	in plane O−C−S bending
ω_5	708.5	S−C−S symmetric stretch	701.9	O−C−S symmetric stretch
ω_6	1385.4	S−C−S asymmetric stretch	1846.5	O−C−S asymmetric stretch

[a] $\omega_3-\omega_6$ correspond to the original four normal modes in the free linear triatomic.

we find that the above reaction is exothermic by 11.7 kJ/mol. Our G-2 method calculations, which are in good agreement with those previously calculated by Curtiss et al.[34] show that the same reaction was endothermic by 42.7 kJ/mol. A similar exercise for the Al + OCS reaction, discussed above, revealed strong agreement between experiment and theory. This led us to question the heat of formation value for the CS radical. Our skepticism about this value was borne out by a literature search, which showed that the heat of formation of carbon monosulfide has been in question for several years. The most recent experimental value of 275 ± 4 kJ/mol by Prinslow et al.[43] gives us a $\Delta H_{rxn} = 31.8$ kJ/mol. Since the agreement between this figure and our calculated value are within the reported error, we have decided to use this experimental heat of reaction. With the exception of an addition mechanism, i.e. formation of an adduct, no exothermic pathway exists for this reaction. The endothermic (20.1 kJ/mol) Al + CO_2 → AlO + CO reaction has been observed to proceed at room temperature.[27] The reaction of aluminum atoms with CO_2 as a function of reactant translational energy has been studied in crossed molecular beams by Costes et al.[44] In these studies, a translational energy threshold of 0.17 eV was observed, as well as an increase in reactive cross section with increasing collision energy, which is characteristic of an endothermic reaction. In our experiments, the production of AlS in the ground vibrational state was verified by an LIF spectrum, despite the relatively large endothermicity. One possible explanation for this result is that only those Al atoms with sufficient energy ($E_{tr} > 0.3$ eV) are reacting to produce AlS. The observed rate constants for the reactions are inconsistent with an abstraction type of mechanism to produce aluminum monosulfide. Much more insight into this process could be gained by carefully examining the dynamics of AlS production.

The rate constant for this reaction at room temperature has been found to be pressure dependent, increasing over the range 5−45 Torr (see Figure 4). The extrapolated zero-pressure rate constant for Al + CS_2 is (4.0 ± 0.8) × 10^{-11} cm^3 molecule^{-1} s^{-1}. We have also calculated a minimum in the potential energy surface corresponding to an AlSCS complex, the structure of which is shown in Figure 5a. The binding energy of the AlSCS stabilized complex is found to be 110.4 kJ/mol, in comparison with that found for $AlCO_2$, 37.7−81.6 kJ/mol.[25,26,29,30] The energy on going from the complex to the products was calculated to be 153.0 kJ/mol. Harmonic frequencies for the Al−CS_2 have also been determined at the MP2 level (see Table 4). As in the Al−OCS case discussed above, addition of an Al atom also causes weakening of the CS bond in carbon disulfide.

Since both the Al−SCS and the Al−OCS complexes have been calculated to have similar structures, we believe it is important to clarify why the former can be stabilized by collisions in the pressure regime measured and the other cannot. One likely explanation is that the barrier to products in the Al−SCS case is greater than on the Al−OCS surface. This arises primarily because the reaction Al + CS_2 → AlS + CS is endothermic, while the analogous Al + OCS→ AlS + CO process is exothermic.

We have also observed the variation in the intercept as a function of pressure for the Al + CS_2 reaction (vide supra). As described above, we believe this arises from forcing a line through a second-order function. As in the OCS case, we did not try to fit our data to higher order functions because the correlation coefficients for the statistical fits were, in general, high. For low pressures (10−20 Torr) and room temperature, we found $r^2 > 0.99$. The observed fits were not as good at high pressure and high temperatures ($r^2 > 0.98$).

The minimum energy structures that we obtained in our ab initio calculations show asymmetrical planar (C_s) configurations for both the Al−CS_2 and Al−OCS species (see Figure 5a,b). No other local minima, corresponding to other structural issues, have been found. Ab initio molecular orbital calculations by Sakai[29] on the Al−CO_2 system predict a more symmetrical (C_{2v}) adduct to be the minimum. Recently, Howard et al. deposited Al atoms in carbon dioxide and carbon disulfide low-temperature matrixes and measured EPR spectra of the corresponding adducts. Their experimental results were in good agreement with the symmetrical (C_{2v}) Al−CO_2 configuration calculated by Sakai.[29] However, their Al−CS_2 results cannot be fit to a C_{2v} type configuration, and they argue that the only alternative structure is consistent with metal atom addition to give SC(Al)S. This spectroscopic finding supports our calculated minimum energy structure.

Summary

We have reported here the first experimental studies of the reaction of ground-state aluminum atoms with triatomic sulfides in the gas phase. These results have been extensively compared with high-level ab initio calculations to reach a detailed understanding of the reaction. Our results and analysis can be summarized as follows.

1. Temperature dependent bimolecular rate constants have been measured for the reactions of Al atoms with OCS and CS_2. In both cases, a slightly negative temperature dependence is observed, consistent with a negligible activation barrier for the reaction of the Al atom.

2. At 298 K, the dependence of the bimolecular rate constants on total pressure has been observed. Only the Al + CS_2 reaction shows pressure-dependent behavior. This result provides experimental verification for the existence of an Al−SCS adduct.

3. Ab initio correlated calculations have been performed to determine the structures of the Al−OCS and Al−CS_2 collision complexes. The existence of a minimum for these adducts is somewhat surprising in the former case in light of the absence of an observed pressure dependence for the bimolecular rate constant. In the case of the latter, the experimentally observed pressure dependent rate constant is consistent with the existence of a metastable adduct.

4. The Gaussian-2 theoretical procedure, based on ab initio correlated methods, has been applied to reactants, products, and complexes in order to evaluate their relative stabilities. For the reactants and products, the calculated results are in strong agreement with previously measured experimental values, with the exception of CS.

While these results and analysis provide a basis of understanding of the studied reactions, they fall short of a complete mechanistic picture. Further ab initio calculations are currently under way in our laboratory in order to determine the structure of the transition state(s) of each reaction. Experimentally, the vibrational and rotational state distributions of the AlS product are being observed under single-collision conditions to further interrogate the dynamics of these reactions.

Acknowledgment. We would like to thank Dr. Fei Wu for his assistance during the experiments, Dr. K. Ravichandran, Dr. H. H. Nelson, and Dr. N. L. Garland for many helpful discussions, and Vivian Rivera and Stephen Gómez for their technical support. We also acknowledge the support of the NSF-EPSCoR and NIH-RCMI programs, for their contributions to the Puerto Rico Laser and Spectroscopy Facility, where the experiments were performed. M.R.P. acknowledges the financial support of the NASA through Grants NAGW-4059 and NCCW-0056. Partial support of this research has also been provided by the U.S. Department of Energy (Grant No. DE-FGO2-94ER75764).

References and Notes

(1) Kurakado, M.; Takahashi, T.; Matsumura, A. *Appl. Phys. Lett.* **1990**, *57*, 1933; Patel, N. G.; Fischer, A. G. *Thin Solid Films* **1988**, *162*, 263.

(2) Sutton, G. P. *Rocket Propulsion Elements*; John Wiley & Sons: New York, 1986.

(3) Muetterties E. L.; Krause, M. J. *Angew. Chem.* **1983**, *95*, 135.

(4) See for example, LeQuere, A. M.; Xu, C.; Manceron, L.; Burkholder, T. R.; Andrews, L. *Gas-Phase Metal Reactions;* Fontijn A., Ed.; Elsevier: Amsterdam, 1992.

(5) Zolensky, M. E.; Mucay, D. S.; Kaczor, L. A. *J. Geophys. Res.* **1989**, *94*, 1047; Brownlee, D. E.; Ferry, G. V.; Tomandl, *D. Science* **1976**, *191*, 1270. Ploeg, T. V.; Zolensky, M. E. *Eos Trans.* **1985**, *66*, 826.

(6) Sridharan, U. C.; DiGiuseppe, T. G.; McFadden, D. L.; Davidovits, P. *J. Chem. Phys.* **1979**, *70*, 5422 .

(7) DiGiuseppe, T. G.; Davidovits, P. *J. Chem. Phys.* **1981**, *74*, 3287.

(8) DiGiuseppe, T. G.; Estes, R.; Davidovits, P. *J. Chem. Phys.* **1982**, *86*, 260.

(9) Tabacco, M. B.; Stanton, C. T.; Sardella, D. J.; Davidovits, P. *J. Chem. Phys.* **1985**, *83*, 5595.

(10) Nemukhin, A. V.; Serebrennikov, L. V. *Usp. Khim.* **1993**, *62*, 566.

(11) Burkholder, T. R.; Andrews, L. *J. Chem. Phys.* **1991**, *95*, 8697.

(12) Burkholder, T. R.; Andrews, L. *J. Phys. Chem.* **1992**, *96*, 10195.

(13) Andrews, L.; Hassanzadeh, P.; Martin, J. M. L.; Taylor, P. R. *J. Phys. Chem.* **1993**, *97*, 5839.

(14) Hassanzadeh, P.; Hannachi, Y.; Andrews, L. *J. Phys. Chem.* **1993**, *97*, 641.

(15) Andrews, L.; Hassanzadeh, P.; Burkholder, T. R. *J. Chem. Phys.* **1993**, *98*, 922.

(16) Burkholder, T. R.; Andrews, L.; Bartlett, R. J. *J. Phys. Chem.* **1993**, *97*, 3500.

(17) Tague, T. J., Jr.; Andrews, L. *J. Am. Chem. Soc.* **1994**, *116*, 4970.

(18) Martin, J. M. L.; Taylor, P. R.; Hassanzadeh, P.; Andrews L. *J. Am. Chem. Soc.* **1993**, *115*, 2510.

(19) Hannachi, Y.; Hassanzadeh, P.; Andrews L. *J. Phys. Chem.* **1994**, *98*, 6950.

(20) Oblath, S. B.; Gole, J. L. *J. Chem. Phys.* **1979**, *70*, 581. Kurtz, H. A.; Jordan K. D. *J. Am. Chem. Soc.* **1980**, *102*, 1177. Mitchell, S. A.; Simard, B.; Rayner, D. M.; Hackett, P. A. *J. Phys. Chem.* **1988**, *92*, 1655. Parnis, J. M.; Mitchell, S. A.; Rayner, D. M.; Hackett, P. A. *J. Phys. Chem.* **1988**, *92*, 3869.

(21) Mitchell, S. A.; Hackett, P. A.; Rayner, D. M.; Cantin, M. *J. Phys. Chem.* **1986**, *90*, 6148.

(22) Perov, P. A.; Shevel'kov, V. F.; Mal'tsev, A. A. *Vestn. Mosk. Univ. Khim.* **1975**, *30*, 109. Hauge, R. H.; Kauffman, J. W.; Margrave, J. L. *J. Am. Chem. Soc.* **1980**, *102*, 6005. Hatton, W. G.; Hacker, N. P.; Kasai, P. H. *J. Phys. Chem.* **1989**, *93*, 1328.

(23) Kelsall, B. J.; Carlson, K. D. *J. Phys. Chem.* **1980**, *84*, 951.

(24) Fontijn, A.; Felder, W. *J. Chem. Phys.* **1977**, *67*, 1561.

(25) McQuaid, M.; Woodward J. R.; Gole, J. L. *J. Phys. Chem.* **1988**, *92*, 252.

(26) Parnis, J. M.; Mitchell, S. A.; Hackett, P. A. *Chem. Phys. Lett.* **1988**, *151*, 485.

(27) Garland, N. L; Douglass, C. H.; Nelson, H. H. *J. Phys. Chem.* **1992**, *96*, 8390.

(28) Le Quéré, A.M.; Xu, C.; Manceron, L. *J. Phys. Chem.* **1991**, *95*, 3031.

(29) Sakai, S. *J. Phys. Chem.* **1992**, *96*, 131.

(30) Selmani, A.; Ouhlal, A. *Chem. Phys. Lett.* **1992**, *191*, 213.

(31) Howard, J. A.; McCague, C.; Sutcliffe, R.; Tse, J. S.; Joly, H. A. *J. Chem. Soc., Faraday* Trans. **1995**, *91*, 799.

(32) Barnhard, K. I.; Santiago, A.; He, M.; Asmar, F.; Weiner, B. R. *Chem. Phys. Lett.* **1991**, *178*, 150.

(33) Frisch, M. J.; Trucks, G. W.; Schlegel, H. B.; Gill, P. M. W.; Johnson, B. G.; Robb, M. A.; Cheeseman, J. R.; Keith, T. A.; Petersson, G. A.; Montgomery, J. A.; Raghavachari, K.; Al-Laham, M. A.; Zakrzewski, V. G.; Ortiz, J. V.; Foresman, J. B.; Cioslowski, J.; Stefanov, B. B.; Nanayakkara, A.; Challacombe, M.; Peng, C. Y.; Ayala, P. Y.; Chen, W.; Wong, M. W.; Andres, J. L.; Replogle, E. S.; Gomperts, R.; Martin, R. L.; Fox, D. J.; Binkley, J. S.; Defrees, D. J.; Baker, J.; Stewart, J. P.; Head-Gordon, M.; Gonzalez, C. and Pople, J. A. *Gaussian 94 (Revision A.1)*; Gaussian, Inc.: Pittsburgh PA, 1995.

(34) Curtiss, L. A.; Raghavachari, K.; Trucks, G. W.; Pople, J. A. *J. Chem. Phys.* **1991**, *94*, 7221.

(35) Zahang, Y.; Stuke, M. *Met. Res. Soc. Symp. Proc.* **1988**, *131*, 375; Zhang, Y.; Stuke, M. *J. Cryst. Growth*, **1988**, *93*, 143.

(36) Moore, C.E. Atomic Energy Levels, NSRDS NBS No. 35, U.S. Govt. Printing Office, Washington, DC, 1971.

(37) He, M.; Wang, H.; Weiner, B. R. *Chem. Phys. Lett.* **1993**, *204*, 563.

(38) Salzberg, A. P.; Santiago, D. I.; Asmar, F.; Sandoval, D. N.; Weiner, B. R. *Chem. Phys. Lett.* **1991**, *180*, 161.

(39) Lide, D. R.; Kehiaian, H. V. *CRC Handbook of Thermophysical and Thermochemical Data*; CRC Press Inc.: Boca Raton, FL, 1994.

(40) Levine, R. D.; Bernstein, R. B. *Molecular Reaction Dynamics and Chemical Reactivity*; Oxford University Press: New York, 1987.

(41) Okabe, H. *Photochemistry of Small Molecules*; John Wiley and Sons: New York, 1978; p 216.

(42) Mitchell, S. A.; Lian, L.; Rayner, D. M.; Hackett, P. A. *J. Chem. Phys.* **1995**, *103*, 5539.

(43) Prinslow, D. A.; Armentrout, P. B. *J. Chem. Phys.* **1991**, *94*, 3563.

(44) Costes, M.; Naulin, C.; Dorthe, G.; Vaucamps, C.; Nouchi, G. *Faraday Discuss. Chem. Soc.* **1987**, *84*, 75.